SIMULATION OF SPACE WEATHERING BASED ON MIE THEORY.

A. Grumpe[1], K. S. Wohlfarth[1], and C. Wöhler[1], [1]Image Analysis Group, TU Dortmund University, Germany {kay.wohlfarth,arne.grumpe,christian.woehler}@tu-dortmund.de

Introduction: Space weathering processes cause the formation of small spherical iron particles in the upper layers of a planetary regolith, termed submicroscopic iron (SMFe) [1]. The presence of this iron results in considerable changes of the observed infrared spectra, i.e., darkening (less reflectance), reddening (increasing slope) and feature obstruction (flattening of spectral features). For remote sensing applications, especially for spectral unmixing procedures, it is of valuable interest to compensate for these effects. This work contributes in three ways: Firstly, the scattering behavior of spherical submicoscopic iron particles is simulated using Mie theory. Based on this, the single scattering albedo, the efficiencies, and the Legendre coefficients of the phase function of SMFe are obtained. Secondly, similar to [2] Hapke's reflectance model [3] is applied to simulate mixtures of silicates with SMFe. This is essentially the simulation of space-weathered particulate surfaces. Thirdly, we have a model for SMFe at hand which can be fed into unmixing procedures to compensate for the known effects of space weathering on the measured spectra. In contrast to [2], the proposed Mie scattering based framework allows for material specific phase functions and arbitrary particle size distributions.

Methods: Space weathering effects have to be considered when evaluating infrared spectra of the soil of an airless planetary body. In order to simulate the effects of space weathering, especially those arising from SMFe, the work of [1] and [2] relies on the Maxwell Garnett theory. Instead of using an effective medium theory, we choose direct modelling of the scattering behavior based on Mie theory. This enables us to carry out calculations with any desired grain size and grain size distribution.

Efficiencies and albedo from Mie therory

Following [3], the extinction efficiency Q_{ext} and the scattering efficiency Q_{sca} are given by

$$Q_{ext}(\lambda) = \frac{2}{x^2}\sum_{n=1}(2n+1)\,\mathrm{Re}(a_n(\lambda)+b_n(\lambda))$$

$$Q_{sca}(\lambda) = \frac{2}{x^2}\sum_{n=1}(2n+1)(|a_n(\lambda)|^2|b_n(\lambda)|^2)$$

The wavelength-dependent single scattering albedo $w(\lambda)$ is the ratio of Q_{sca} and Q_{ext}. The quantities a_n and b_n are termed Mie coefficients and are calculated according to [4] and [5] from the refractive index.

Legendre Expansion of Mie Phase Function As described by [4], the phase function $p(g)$ of a spherical particle is given by the sum of the squared absolute value of the scattering matrix's diagonal elements S_1 and S_2. The aim is to find a Legendre representation with Legendre coefficients χ_n.

$$p(g) = \frac{1}{k^2R^2}\frac{|S_1(g)|^2+|S_2(g)|^2}{2} = \sum_{k=0}^{N}\chi_n P_n(\mu)$$

Employing the derivations of [6] yields the Legendre coefficients h_{n11} and h_{n22} of S_1 and S_2, respectively. The n^{th} Legendre coefficient of the phase function is finally

$$\chi_n = \frac{(2n+1)}{2k^2R^2}(h_{n11}+h_{n22})$$

Reflectance Modelling and Spectral Mixing. The approach of Hapke [3] is a well established way to model the reflectance behavior of particulate surfaces. The model requires the illumination conditions, the wavelength dependent single scattering albedo, and the phase function of a particulate material in Legendre representation.

Simulation. The mixing procedure falls into 4 parts. (1a) Measured reflectance spectra of selected minerals are utilized in order to retrieve the single scattering albedo spectrum w_i of the i-th given material by non-linear optimization. (1b) Mie theory is employed for calculating the w spectrum of SMFe particles. (2) Given the mass fractions and the scattering efficiencies, the spectra w_i are combined to the new albedo w by linear mixing [1, 3]. (3) Based on the mass fractions and the Legendre coefficients of the minerals under investigation, the phase functions $p_i(g)$ are weighted with the albedo w and mixed in a linear fashion. (4) The mixed albedo w and the mixed phase function $p(g)$ are inserted into the Hapke model, generating the final radiance spectrum.

The expected amount of iron on Mercury's surface is subject to the current debate. In [7], the conclusion is drawn that the amount of iron on Mercury considerable less than on the moon. Contrary to that, [8] argue that there is more SMFe on the Mercurian surface than on the moon. Thus, we choose to simulate up to 1 wt% of iron, which is roughly two times the amount of iron that is present on the moon.

Results: For our experiments, we use measured radiance spectra of olivine particles of an average radius of 47.5 µm and mix it with simulated SMFe of 0.01 µm in radius.

In the visible and the near infrared region, we used the refractive index of olivine from [9] and of iron from [10] and plot six mixtures with an iron mass percentage of 0% - 1 % . The incidence angle is *i*=15° and the emission angle is *e*=15°. As it can be seen in Figure 1, the three prominent effects of space weathering i.e. darkening, reddening, and feature obstruction, get stronger with increasing iron content.

In the mid infrared region, we use the refractive index measurements of olivine [11] and iron [10] and plot mixtures with 0% - 1% weight percent of iron (Figure 2). For the TIR region, we can observe that the space weathering effects effects become less prominent. The diagnostic Restrahlenband and the Christiansen feature are only slightely affected.

References: [1] Hapke B. (2001) *Journal of Geophysical Research*, 106, 10,039–10,073. [2] Warell J. et al. (2009) *Icarus*, 209, 164-178. [3] Hapke B. (2002) *Icarus*, 157, 523–534. [4] de Rooij W. A. et al. (1984) *Astronomy and Astrophysics*, 131, 237–248. [5] Mätzler C. (2002) *Research Report, Institute of Applied Physics*, University of Bern. [6] Fowler B. (1983) *Journal of the Optical Society of America*, 73, 19–22. [7] Warell J. (2010) *Icarus*, 209(1), 138-163. [8] Sato H. et al. (2014) *J. Geophys. Res. Planets*, 119, 1775–1805. [9] Trang D. et al. (2013) *Journal of Geophysical Research*, 118,708-732. [10] Querry M.R. (1985) *Contractor Report CRDC-CR-85034 (1985)*. [11] Laboratory Astrophysics Group AIU Jena (2002)

.

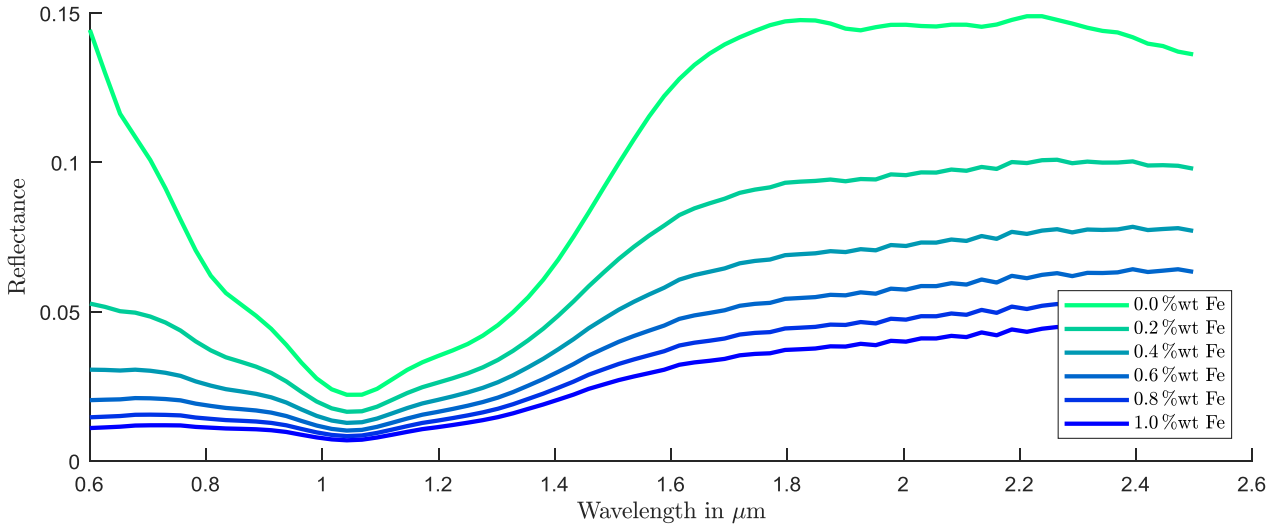

Figure 1: Simulation of space-weathered olivine in NIR

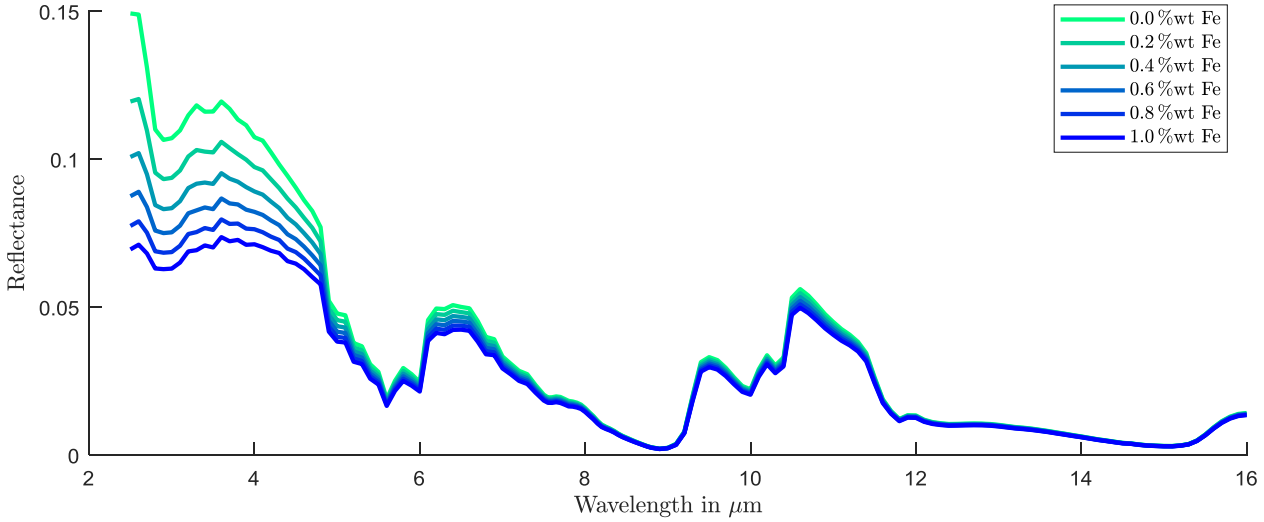

Figure 2: Simulation of space-weathered olivine in TIR